

A study on electrodeposited $\text{Ni}_x\text{Fe}_{1-x}$ alloy films

M BEDIR^{1,*}, Ö F BAKKALOĞLU, İ H KARAHAN² and M ÖZTAŞ

¹Department of Engineering Physics, University of Gaziantep, 27310-Gaziantep, Turkey

²Department of Physics, Faculty of Science and Arts, University of Gaziantep, Kilis, Turkey

*Corresponding author. E-mail: bedir@gantep.edu.tr

MS received 16 September 2005; revised 20 December 2005; accepted 15 March 2006

Abstract. $\text{Ni}_x\text{Fe}_{1-x}$ ($0.22 \leq x \leq 0.62$) alloy films were grown by electrodeposition technique. A shift in diffraction peaks of NiFe and Ni_3Fe was detected with increasing Ni content. The highest positive magnetoresistance ratio was detected as 5% in $\text{Ni}_{0.51}\text{Fe}_{0.49}$. Positive and negative anisotropic magnetoresistance were observed in longitudinal and transverse geometries respectively. The highest anisotropic magnetoresistance ratio of 9.8% was also detected in $\text{Ni}_{0.51}\text{Fe}_{0.49}$. The angular variation of magnetoresistance was studied. Magnetisation loop curves show that NiFe alloy films have a linear decreasing anisotropy constant with increasing Ni deposit content and show a decreasing behavior of coercivity which indicates soft magnetic property with increasing Ni deposit content.

Keywords. Magnetic films; electrodeposition; X-ray diffraction; magnetoresistance; magnetic measurement.

PACS Nos 75.70; 72.15.G; 81.15.L; 75.50.C

1. Introduction

Metallic alloy films, which are composed of magnetic–nonmagnetic or magnetic–magnetic elements, have regained attention over the past decade due to their magnetic and magnetoresistive properties. The properties of magnetoresistive systems are closely related to their constituent elements and their structures. The conduction electron motion in a magnetic–magnetic system may therefore be affected in a more different way than that in a magnetic–nonmagnetic system. Giant magnetoresistance effect which is an isotropic effect, and anisotropic magnetoresistance effect which is a direction-dependent effect, are observed in both types of systems. CuCo [1,2], NiCu [3], FeCu [4] systems are examples of the magnetic–nonmagnetic magnetoresistive systems while NiFe alloy system is among the magnetic–magnetic systems composed of high magnetic moments. NiFe systems generally show anisotropic magnetoresistance properties [5–8]. Investigations on the magnetic and magnetoresistance properties of NiFe alloy films are mostly focused on the properties of $\text{Ni}_{81}\text{Fe}_{19}$ permalloy systems. However, there are fewer

studies on thin films of NiFe systems (which are generally around or less than nanometric scale in thickness) with varying compositions prepared by using different techniques.

NiFe systems are fabricated in the forms of alloys, multilayers and nanowires using different deposition techniques such as evaporation, sputtering, molecular beam epitaxy and electrodeposition. Each deposition technique has different advantages over others. Different techniques may cause the films to have different structural and therefore different physical properties. Electrodeposition, which is a relatively cheap technique, does not need any sophisticated equipment and may easily be employed to grow NiFe alloy films with different properties by controlling electrodeposition variables. Several techniques such as X-ray diffraction [9], VSM [10], Mössbauer spectroscopy [11], four-point probe [12] etc. are used to investigate the crystallographic, magnetic and magnetotransport properties of NiFe systems.

In this study our aim is to prepare NiFe alloy films relatively thicker (in μm scale) than those reported in literature, with different compositions using electrodeposition technique and to investigate their structural-, magnetic- and directional-dependent magnetoresistance properties of NiFe films.

2. Experimental details

$\text{Ni}_x\text{Fe}_{1-x}$ films were electrodeposited at room temperature from a sulfate bath. In the bath, Ni^{2+} concentrations were varied from 0.0025 to 0.11 M, while the Fe^{2+} concentrations were kept at 0.02 M. The other component in the bath solution was 0.4 M H_3BO_3 . The pH value of the solution was adjusted to 3 with 1 M H_2SO_4 solution. The bath solution was freshly prepared before each deposition. The deposition was performed in the constant current mode ($16 \text{ mA}/\text{cm}^2$) with two electrode configurations. The substrate was a copper plate while a platinum electrode was used as anode. Because the adhesion of NiFe alloy film onto Cu substrate is very good, we avoided any organic addition to the bath in order to keep organic contamination as minimum as possible within the film and also no stirring was performed to obtain a film prepared without mechanical intervention to the deposition. The Cu substrates were first mechanically and then electrochemically polished in a phosphoric acid solution until a mirrorlike appearance was obtained. The NiFe films were stripped from their substrates in a chromic-sulfuric acid solution.

The compositions of the films were determined using an atomic absorption spectrophotometer. Using the atomic absorption results, the thicknesses of the films were calculated to be ranging from ~ 2.3 to $\sim 3 \mu\text{m}$. The crystal structures of the films were analysed by X-ray (Cu K_α) diffraction method. The four-point probe method was used to measure the resistivity and magnetoresistance effect in (i) the longitudinal magnetoresistance geometry and (ii) the transverse magnetoresistance geometry. Magnetoresistance was also measured with the variation of angle from parallel to perpendicular geometries. Magnetisation loop spectra were taken with the magnetic field applied parallel and perpendicular to the film plane using a vibrating sample magnetometer at room temperature. The dimensions of the films used in the magnetoresistance and VSM measurements were $4 \text{ mm} \times 4 \text{ mm}$.

3. Results and discussion

3.1 Sample characterisation

Figure 1 shows the dependence of Ni deposit content on the bath Ni^{2+} ion concentration. The concentration of Fe^{2+} ions in all the baths is taken as 0.02 M. It is clear from the figure that the Ni deposit content is measured to be 42 wt% for the bath Ni^{2+} concentration of $M = 0.02$ while the Fe deposit content is obtained to be 58 wt%. The increase in the Ni deposit content is relatively sharp for low Ni^{2+} concentration (<0.0126 M) but it continues with a lower slope for higher Ni^{2+} concentrations.

The standard electrode potential of pure Ni^{2+} (-0.257 V) is relatively more positive than that of Fe^{2+} (-0.44 V). An element with a higher positive standard electrode potential is normally expected to deposit preferentially than the one with a less positive standard electrode potential. However, the results in figure 1 indicate that the Fe^{2+} ions are preferentially deposited than the Ni^{2+} ions although the reverse is expected. This is attributed to the phenomenon called ‘anomalous codeposition’ which is described as the preferential deposition of the element with less positive standard electrode potential [13]. The concentration of Ni^{2+} and Fe^{2+} ions in the neighborhood of substrate may instantaneously change due to the anomalous Fe deposition. This may result in the creations of Fe-rich and Ni-rich regions in these films in the absence of any stirring during deposition although Fe and Ni atoms are miscible in NiFe alloy.

Figure 2 shows an example of X-ray diffraction spectra of NiFe films. The peak at $2\theta = 44-44.5^\circ$ represents the diffraction from (1 1 1) plane of fcc structure while the diffraction angle ($2\theta = 43.6^\circ$) of the other smaller peak corresponds to Ni_3Fe . The crystal structure of Ni_3Fe is called a superlattice structure which has a cubic crystal structure composed of three Ni atoms each of which is located at the center of each cubic face and an Fe atom placed at the corners of the cube [14]. Similar diffraction peaks of Ni_3Fe were also reported in electrodeposited Au/NiFe/Cu [15], in sputtered NiFeCo–Ag films [16] and in Ni_3Fe powder [17]. It is observed that both the peaks shift to lower angles with decreasing amount of Ni content in the samples. The broad linewidth of the (1 1 1) peak may indicate that it is contributed by a distribution of different sized grains in the electrodeposited films. When the

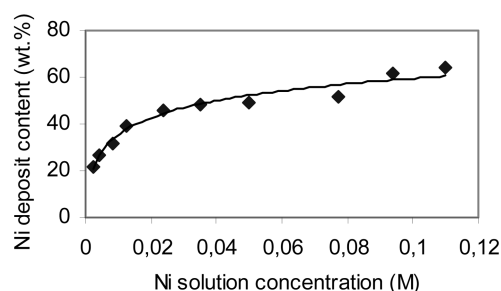


Figure 1. Dependence of Ni deposit content on Ni solution concentration.

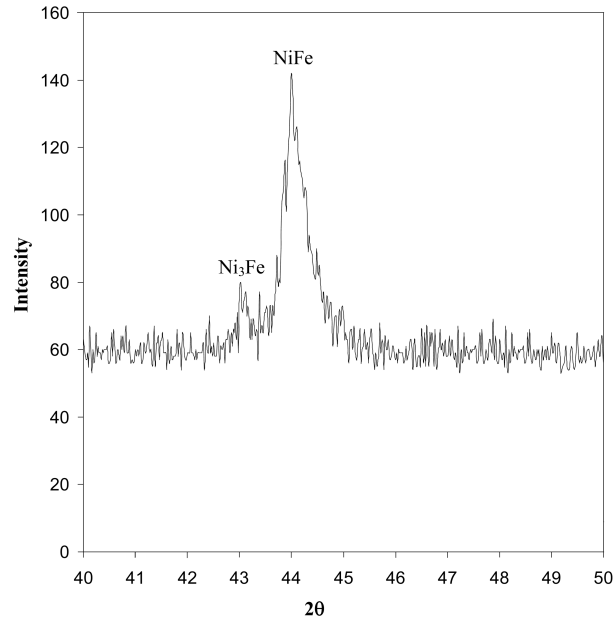


Figure 2. An example of X-ray diffraction spectra of $\text{Ni}_{0.46}\text{Fe}_{0.54}$ film.

deposit Ni content has a value of about 22% (or in other words, 78% Fe content), the peaks shifted back to the high angle side indicating the start of domination of bcc structure at this composition.

3.2 Magnetoresistance measurements

Magnetoresistance is described as the influence of magnetic field on the resistivity of a material. In the case of a nonmagnetic material, it is named as ‘the ordinary magnetoresistance’. When a material is magnetic, a larger magnetoresistance effect is observed, which is attributed to the magnetic properties of the sample. The presence of magnetic entity may be seen to contribute to the magnetoresistance of a material in two ways: (i) anisotropic contribution and (ii) giant magnetoresistance. In the anisotropic case, the magnetoresistance effect depends on the relative orientation of the magnetic field and current directions. When the magnetic field is applied parallel to the electric current, the magnetic domains rotate to form a single one with the magnetisation vector aligned along the applied field direction. This usually results in an increase in the resistivity which is called the longitudinal magnetoresistance. When the magnetic field is applied perpendicular to the current, a decrease in resistivity is observed as domains align themselves in a single form with the magnetisation vector perpendicular to the applied field. This magnetoresistance effect is named as the transverse magnetoresistance effect. The difference between the longitudinal and transverse effect is defined as the anisotropic effect and it is considered to be the effect of magnetisation alignment on to the resistivity of a magnetic sample. In the case of giant magnetoresistance a large decrease in

resistivity with increasing magnetic field is observed. The giant magnetoresistance effect is the result of the spin scattering generally at the interfaces of grains and layers and it is an isotropic effect, i.e. it is independent of the applied field direction.

It is reported that the films and bulk material of NiFe alloy systems generally exhibit anisotropic magnetoresistance (AMR) effect [18,19]. The AMR effect is also observed in the nanowire of NiFe alloy films [20]. The giant MR (GMR) effect is usually detected in the multilayer form of those films (e.g. in FeNi/Cu [12] and NiFe/Ag films [21]). The resistivity of NiFe system is reported to depend closely on the film composition, e.g. the resistivity values of $Ni_{30}Fe_{70}$ and $Ni_{80}Fe_{20}$ systems are obtained to be $\sim 85 \mu\Omega\text{-cm}$ and $\sim 9 \mu\Omega\text{-cm}$ respectively [22].

In our study, the four-point probe method was employed in the measurement of electrical resistivity and magnetoresistance effect. The thermal voltage effect was eliminated by taking the average of voltage readings with two reverse currents in each configuration described below. Figure 3 shows the electrical resistivity variation with the composition of our NiFe samples. The resistivity of the films decreases from $89 \mu\Omega\text{-cm}$ to $17 \mu\Omega\text{-cm}$ with the Ni increase from 22 to 64%. This decrease is in good agreement with that reported in [22]. The highest resistivities ($\sim 90 \mu\Omega\text{-cm}$) in our films are detected in the films whose diffraction peaks shift back to the higher angle side with decreasing Ni content as described above. This result implies that the relative number of scattering centers in the NiFe films increases with decreasing Ni content in the film. The resistivity of the NiFe films with low Ni (high Fe) content ($< 22\%$) could not be measured due to the stress-crack formation in deposits.

Magnetoresistance ratio is described as $\Delta R/R = [R(H) - R(0)]/R(0)$, where $R(H)$ and $R(0)$ are respectively the resistances in the presence and absence of the applied magnetic field. In the longitudinal geometry, the current was directed parallel to the magnetic field which was applied parallel to the film plane. Some examples of the longitudinal magnetoresistance (LMR) curves of the NiFe samples of various compositions are shown in figure 4. In all the samples in the longitudinal geometry, it is observed that the resistance sharply increases with a relatively small magnetic field increment (~ 200 Oe). The increase in resistance with magnetic field results in a magnetoresistance named as positive or longitudinal magnetoresistance

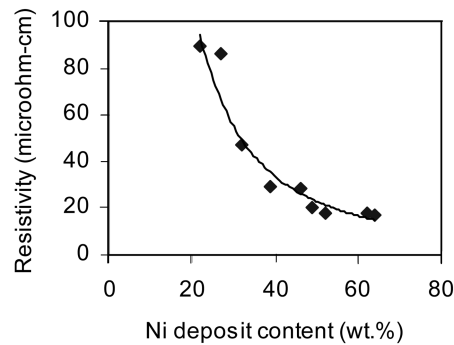


Figure 3. Electrical resistivity variation with the composition of the NiFe samples.

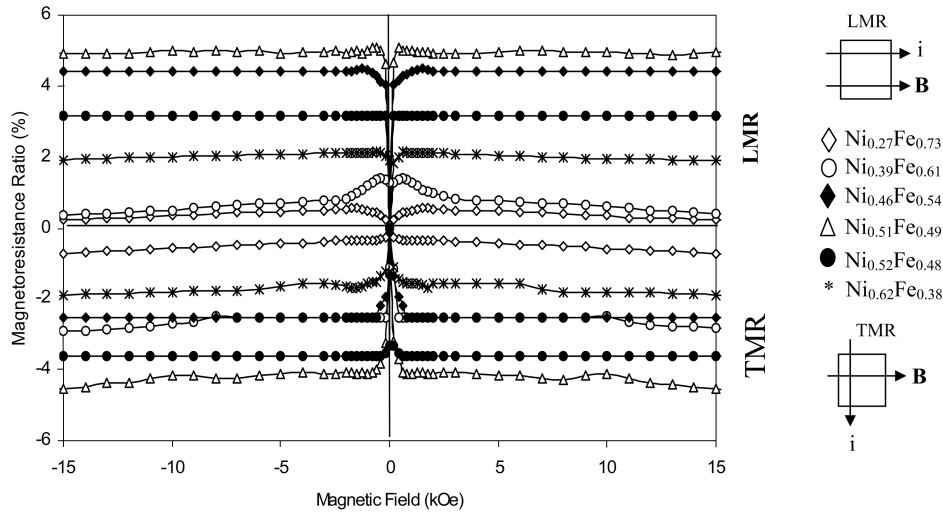


Figure 4. Longitudinal and transverse magnetoresistance (magnetoresistance ratio) curves of NiFe samples.

effect. The maximum positive MR value is observed as 5% in the sample with Ni content of $x = 0.51$ while the lowest value is 0.6% in the sample of $x = 0.27$. The positive MR of the samples with $x = 0.46, 0.51$ and 0.52 becomes constant whereas the positive MR values of the other samples decrease with increasing magnetic field above 200 Oe (figure 4). The initial sharp increase in the positive magnetoresistance effect (or in the resistance) for a small magnetic field increment (below ~ 200 Oe) is due to the domain wall motion and the rotation of magnetisation vector. The decrease in the resistance above a certain magnetic field value is due to the forced increase of spontaneous magnetisation caused by the application of a strong magnetic field. The forced decrease of resistance is attributed to a less 4s electron scattering in the Mott's and Kasuya's theories [22]. The slope in the decrease of MR effect in strong fields may reflect the rate of decrease of 4s electron scattering. The constant LMR in the samples with $x = 0.46, 0.51$ and 0.52 above ~ 200 – 1000 Oe indicates no more unmeasurable decrease in the 4s electron scattering. The slope in the decrease of the positive MR effect (or in the resistivity) in the samples with $x = 0.22, 0.27, 0.39, 0.62$ and 0.64 above >1000 Oe is between $-8.4 \times 10^{-3} \%$ /kOe (for $x = 0.48$) and -0.04% /kOe (for $x = 0.39$). No saturation was obtained even in the magnetic field of 20 kOe in these samples. Another feature seen in the LMR measurements is that the maximum value of the positive MR effect depends on the compositions of the samples. The maximum values of positive MR effect with Ni content of $x \geq 0.46$ are between 2 and 5% while the values for the samples with lower Ni content of $x < 0.46$ are between 0.6 and 1.4%. It is reported that for pure Ni, the maximum positive MR is about 2% whereas it is 0.3% for pure Fe [23]. The decrease in the maximum value of positive MR effect with increasing Fe content in our NiFe samples may therefore be attributed to the contribution of the lower positive MR value of Fe rather than that of Ni beside other factors such as grain size change, the degree of ferromagnetic coupling etc.

In the transverse configuration, the direction of the magnetic field was kept the same as in the longitudinal geometry while the direction of current was oriented perpendicular to the magnetic field in the film plane. The application of a magnetic field in the transverse geometry causes a decrease in the resistance and this effect is called a negative magnetoresistance or transverse magnetoresistance (TMR) effect. In all the samples a sharp decrease in the resistance is detected at low fields as can be seen from the examples of the transverse MR curves in figure 4. The negative MR effect in the samples with $x = 0.46$ and 0.52 becomes constant above ~ 200 Oe while in the other samples with $x = 0.22, 0.27, 0.39, 0.48, 0.51, 0.62$ and 0.64 , the increase in the negative MR effect with increasing field continued with a slope between $-0.018\%/kOe$ (for $x = 0.62$) and $-0.031\%/kOe$ (for $x = 0.48$ and 0.52). The increase in the negative MR with high fields in these samples is again due to the approach of magnetisation to a more complete saturation, indicating additional less 4s electron scattering. It is found in the MR measurements of the TMR geometry that the maximum value of MR ratio is also composition-dependent so that it is between 1.5 and 5% in the samples with the Ni percentage concentration ≥ 0.46 and between 0.8 and 1.4% in the samples with $x < 0.39$ at 20 kOe. Again a similar comment, based on the difference in the MR values of pure Ni and pure Fe, as done for the composition dependency of the LMR geometry may be valid for the composition dependency of the negative MR effect measured in the TMR geometry in the NiFe alloy films.

Anisotropic magnetoresistance is frequently expressed as the difference between LMR and TMR [24]. Figure 5 shows the AMR values measured at 200 Oe as a function of Ni content in our samples. The highest value of AMR is observed as 9.8% in the $Ni_{0.51}Fe_{0.49}$ sample which is one of our low resistive samples (see figure 3) and the lowest AMR value was 0.9% in $Ni_{0.27}Fe_{0.73}$ which is one of our high resistive samples whereas the bulk NiFe alloy exhibits an AMR of 5% at a composition of $\sim 90\%$ Ni and 10% Fe [22]. Our highest AMR value of 9.8% observed in the $Ni_{0.51}Fe_{0.49}$ sample corresponds to the same AMR value observed in an electrodeposited NiFe film with a different composition of 85% Ni and 15% Fe reported by

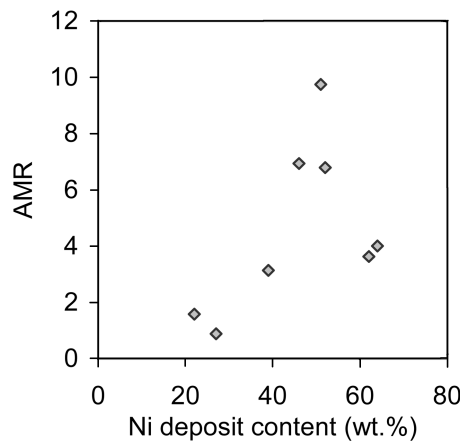


Figure 5. Variations of anisotropic magnetoresistances with Ni content.

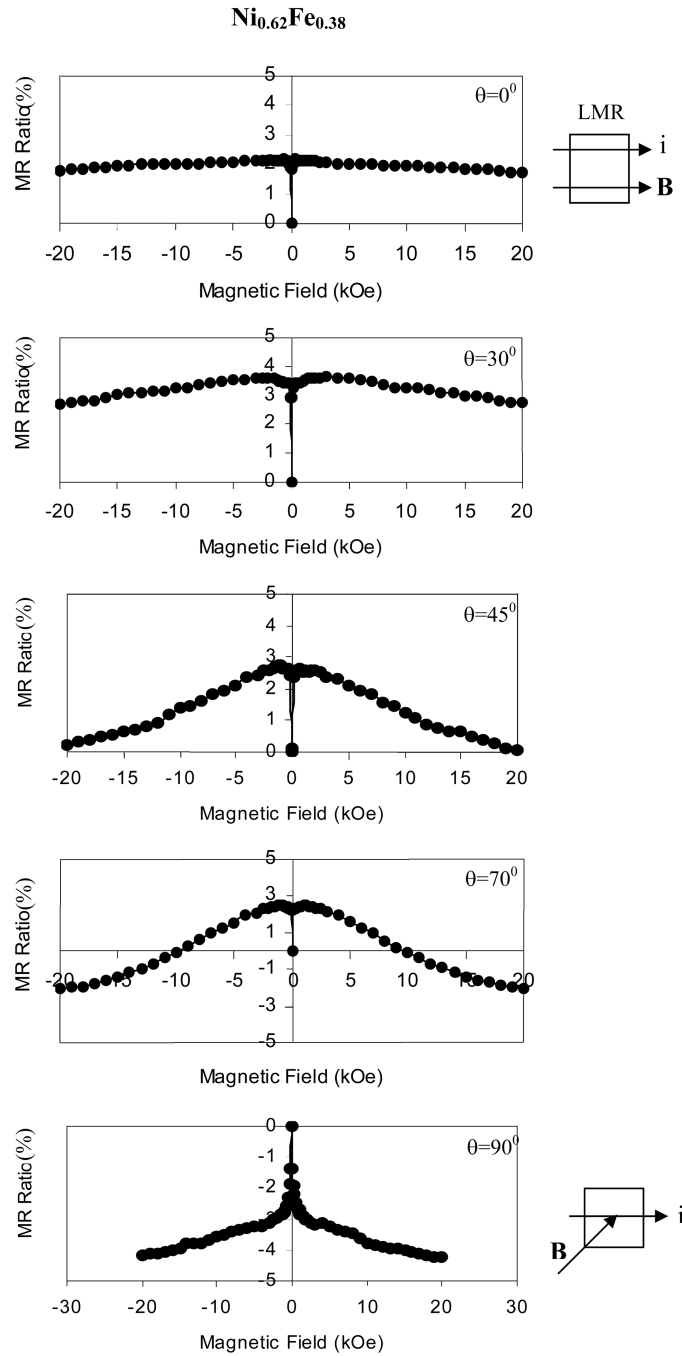


Figure 6. An example of the angular variation of MR curves in the Ni_{0.62}Fe_{0.38} alloy film, where θ is the angle between the applied field and film plane and varied from 0° longitudinal to 90° perpendicular geometry.

Myung and Nobe [8]. The origin of the AMR is attributed to the spin-orbit coupling. McGuire and Potter [7] however reported that AMR changed significantly depending on thickness, grain size and deposition parameters. O'Handley [25] also reports that the AMR values of pure Ni, Co, Fe and Ni_3Fe systems show a departure from the general trend of AMR vs. Bohr magneton curve of Ni-based (NiFe, NiCo, NiCu, NiFeCu) alloys. The MR results of our electrodeposited NiFe films which contain a Ni_3Fe component, suggest that the highest effect of the spin-orbit coupling is seen in the low resistive $Ni_{0.51}Fe_{0.49}$ film among others.

As an example which we could not encounter in literature, the angular variation of MR curves from 0 to 90° was examined in a geometry in which the magnetic field was varied from a parallel position to a perpendicular position to the film surface while the direction of the current was kept unchanged in the film plane. The change from the pure positive MR effect to the negative MR effect with the gradual change in the direction of applied field from parallel ($\theta = 0^\circ$) to perpendicular ($\theta = 90^\circ$) to film plane is clearly seen in figure 6. As the angle between the applied field and the film plane increases, the perpendicular component of the field is created at the expense of the parallel one, and the saturation in the positive MR value is lost while a decreasing effect in the MR ratio emerges. Above 45° the positive MR gradually loses its strength at high fields and a tendency towards a negative MR behavior, indicating a less conduction electron scattering, starts, and eventually gets the negative MR behavior at 90° . It can be seen from figure 6 that the change from positive to negative MR behavior appears to be not abrupt but almost a gradual one.

3.3 Magnetisation measurements

The magnetic anisotropy and coercive fields are important properties of soft magnetic materials which find applications in the magnetic recording and reading technology. We therefore examine the magnetic anisotropy constant and coercive field of our relatively thick electrodeposited NiFe alloy films.

The magnetisation loops of Ni_xFe_{1-x} samples were measured using a vibrating sample magnetometer with a magnetic field applied parallel or perpendicular to the film plane at room temperature. Figure 7 shows an example of magnetisation curves of NiFe films. The perpendicular field M_s - H curves clearly show that the curves are mostly straight lines with a small easy axis hysteresis which occur by domain translation and rotation. This shows that the uniaxial anisotropy, which is dependent on the film microstructure such as grain size, preferred orientation and stress, is mostly confined in-plane. The anisotropy constant K was calculated using the well-known expression $H_k = 2K/M_s$ where H_k is the anisotropy field and M_s is the saturation magnetisation. In the parallel anisotropy constant calculations, the external field H is assumed to be equal to H_k while in the perpendicular case, the demagnetisation field correction was performed using the expression $H_k = H - H_d$ where $H_d = 4\pi M_s$ is the demagnetisation field. The perpendicular (anisotropy) field has a huge value (above 10^4 Oe) when compared with the parallel (anisotropy) field (less than 10^3 Oe), because of the shape anisotropy. The variation of K with Ni content is shown in figure 8. As expected, the perpendicular anisotropy constant is larger than the parallel anisotropy constant. As the Ni content increases,

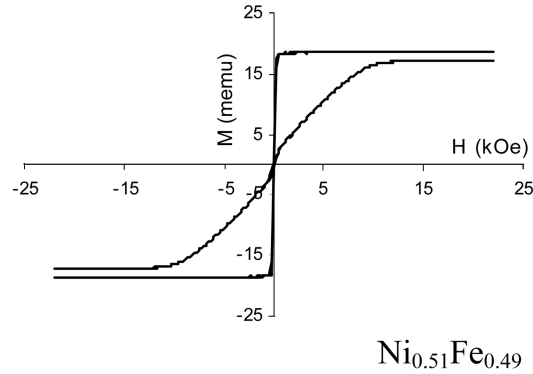


Figure 7. An example of magnetisation curves of NiFe films.

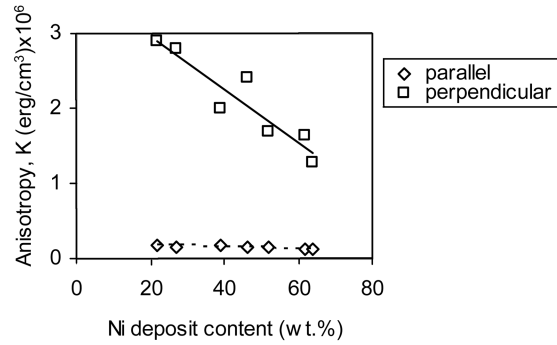


Figure 8. Variations of parallel and perpendicular anisotropy constants K with Ni deposit content.

the anisotropy constant decreases towards zero in both parallel and perpendicular geometries. The decreasing behavior of the anisotropy constant with increasing Ni content may signal the approach of the anisotropy energy surface towards spherical one where the anisotropy constant becomes zero and it is easy to change the direction of magnetisation with an applied field, $H_k \approx 0$.

Coercivity (H_c) and M_r/M_s are dependent on the microstructure of the films including grain size and magnetic order. The M_r/M_s value varies between 7.6% for $\text{Ni}_{0.46}\text{Fe}_{0.54}$ and 42.9% for $\text{Ni}_{0.52}\text{Fe}_{0.48}$ which reflects the degree of the ferromagnetic order of NiFe particles in our samples. The variation of coercive field H_c with Ni content is shown in figure 9. As the Ni content increases H_c decreases for both parallel and perpendicular geometries, which confirms a softer NiFe film with more Ni content.

4. Conclusions

Our relatively thick NiFe alloy films show the NiFe and Ni_3Fe diffraction lines. The highest positive magnetoresistance ratio was detected to be 5% in $\text{Ni}_{0.51}\text{Fe}_{0.49}$.

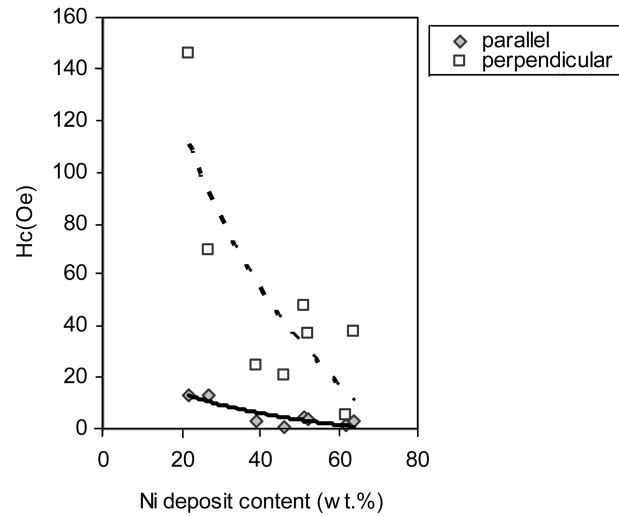


Figure 9. Variation of coercive field H_c with Ni deposit content.

Anisotropic MR effect was detected in all the samples studied in this work. The highest positive AMR was detected to be 9.8% in $Ni_{0.51}Fe_{0.49}$. The variation of the magnetic field from a parallel configuration to perpendicular one resulted in a gradual MR change from positive to negative value. A linear decreasing behavior of the uniaxial anisotropy constant with Ni percentage was determined.

References

- [1] A E Berkowitz, J R Mithchell, M J Carey, A P Young, S Zhang, F E Spada, F T Parker, A Hutten and G Thomas, *Phys. Rev. Lett.* **68**, 3745 (1992)
- [2] G R Pattannaik, S C Kashyap and D K Pandya, *J. Magn. Magn. Mater.* **219**, 309 (2000)
- [3] I Bakonyi, J Tath, L Gounlou, T Becsei, E Toth-Kadar, W Schwarzacher and G Nabiyouni, *J. Electrochem. Soc.* **149**, C195 (2002)
- [4] A J A de Oliveira, W A Ortiz, D H Mosca, N Mattoso, I Mazzara and W H Schreiner, *J. Phys.: Condens. Matter* **11**(1), 47 (1999)
- [5] F C Williams Jr and E N Mitchell, *Jpn. J. Appl. Phys.* **7**, 739 (1968)
- [6] E N Mitchell, H D Haukaas, H D Bale and J B Streep, *J. Appl. Phys.* **35**, 2604 (1964)
- [7] T R McGuire and R I Potter, *IEEE Trans. Magn. Mag-II*, 1018 (1975)
- [8] N V Myung and K Nobe, *J. Electrochem. Soc.* **148**, C136 (2001)
- [9] F Czerwinski, J A Szpunar and U Erb, *J. Mater. Sci.: Mater. Electron.* **11**, 243 (2000)
- [10] F E Rasmusen, J T Ravnkilde, P T Tang, O Hansen and S Bouwstra, *Sensors and Actuators* **A92**, 242 (2001)
- [11] J A Hutchings, K Newstead, M F Thomas, G Sinclair, D E Joyce and P J Grundy, *J. Phys.: Condens. Matter* **11**, 3449 (1999)

- [12] A Siritariwat, E W Hill, I Stutt, J M Fallon and P J Grundy, *Sensors and Actuators* **81**, 40 (2000)
- [13] A Brenner, *Electrodeposition of alloys, principle and practice* (Academic Press, New York, 1963) vol. II, Chap. 31, p. 239
- [14] S Chikazumi, *Physics of magnetism* (John Wiley & Sons, New York, 1964) Chap. 17, p. 361
- [15] I Vitina, M Lubane, A Korne, V Rubene, V Belmane, Z Zarina and A Krumina, *Thin Solid Films* **270**, 380 (1995)
- [16] H Wang, S P Wong, X Lu, X Yan, W Y Cheung, N Ke, S Hu, D Zeng and Z Liu, *J. Phys.* **D33**, 1464 (2000)
- [17] P Bose, S Bid, S K Pradhan, M Pal and D Chakravorty, *J. Alloys and Compounds* **343**, 192 (2002)
- [18] E Rozenberg, A I Shames, G Gorodetsky, J Pelleg and I Felner, *J. Magn. Magn. Mater.* **203**, 102 (1999)
- [19] J Neamtu, M Volmer and A Coraci, *Thin Solid Films* **343–344**, 218 (1999)
- [20] H R Khan and K Petrikowski, *J. Magn. Magn. Mater.* **215–216**, 526 (2000)
- [21] M A Parker, T L Hylton, K R Coffey and J K Howard, *J. Appl. Phys.* **75(10)**, 6382 (1994)
- [22] R M Bozorth, *Ferromagnetism* (Van Nostrand, New York, 1951) p. 745
- [23] B D Cullity, *Introduction to magnetic materials* (Addison-Wesley, Massachusetts, 1972) pp. 284, 526
- [24] E Toth-Kadar, L Peter, T Becsei, J Toth, L Pogany, T Tarnoczi, P Kamasa, I Bakonyi, G Lang, A Cziraki and W Schwarzacher, *J. Electrochem. Soc.* **147**, 3311 (2000)
- [25] R C O'Handley, *Modern magnetic materials, principals and applications* (John Wiley & Sons Inc., New York, 2000) pp.189, 577